

Cellulose/Water: Liquid/Gas and Liquid/Liquid Phase Equilibria and Their Consistent Modeling

John Eckelt and Bernhard A. Wolf*

Institut für Physikalische Chemie der Johannes Gutenberg Universität and Materialwissenschaftliches Forschungszentrum, Universität Mainz, Welder-Weg 13, D-55099 Mainz, Germany

Received February 12, 2007; Revised Manuscript Received April 10, 2007

Liquid/liquid and liquid/gas equilibria were measured for the water/cellulose system at 80 °C using three different polymer samples. For these experiments we prepared cellulose films of approximately 20–25 μm in thickness and determined their equilibrium swelling in water. Thereafter the polymer concentration in the mixed phase was increased by means of a stepwise removal of the volatile component, and the equilibrium vapor pressures were measured using an automated combination of head space sampling and gas chromatography. Contrary to the usual behavior of polymers, the swelling of cellulose increases as its molar mass becomes larger. The Flory–Huggins interaction parameters calculated from the measured vapor pressures pass a pronounced minimum as a function of composition; for high cellulose contents they are negative, whereas they become positive for water-rich mixtures. All experimental findings are consistently interpreted by means of an approach accounting explicitly for the effects of chain connectivity and for the ability of macromolecules to respond to environmental changes by conformational rearrangement.

1. Introduction

The importance of cellulose for chemistry and every day life is beyond doubt. Nevertheless our knowledge on the interactions of this biopolymer with other compounds is far from being satisfying. The most interesting substance in this context is water, not only because of the well-known interaction of cellulose with the moisture of the air, but also for technical purposes, in particular in the context of the Lyocell process, where water constitutes the required precipitant of cellulose from its solutions in *N*-methylmorpholine-*N*-oxide (NMMO).

The capability of cellulose to incorporate large amounts of water is one of its outstanding features and has been known for a very long time. Despite this situation, publications describing the equilibrium swelling of cellulose and the influences of its molar mass on it are to the best of our knowledge still missing. However, considerable labor has been devoted to the study of the kinetics and mechanisms of water sorption as well as to the structural changes induced by water. Some recent examples (containing references to the older work) are quoted. The methods that are being applied in this context include all kinds of NMR techniques,^{1,2} Fourier transform infrared studies,³ sorption procedures,⁴ X-ray scattering methods,⁵ the Knudsen effusion technique,⁶ and even ζ potential measurements.⁷

In this work we wanted to investigate the possibilities for the application of thermodynamic methods that are well established for solutions of synthetic vinyl polymers to the water/cellulose system. To erase to the highest possible extent the dissimilarities in the structures of cellulose samples stemming from different sources, we have first and foremost completely dissolved the polymers in the mixed solvent dimethylacetamide + LiCl. From these solutions we have then prepared thin films (20–25 μm in thickness) to ease the establishment of the thermodynamic equilibria by minimizing diffusion distances of water into the cellulose bulk phase and out of it.

All measurements presented here were performed at 80 °C in view of similar experiments that we are presently performing with the NMMO/water/cellulose system, which require this minimum temperature. The melting point of NMMO monohydrate is somewhat less than 80 °C. The literature data vary between 72,⁸ 75,⁹ or 78 °C.¹⁰ The melting point of anhydrous NMMO is reported to be 184.2 °C.¹¹ In view of the high viscosities of the mixture, temperatures higher than 80 °C would be desirable to attain phase equilibria within reasonable time. However, to avoid degradation during measurement times, which can reach several weeks, we refrained from such experiments.

2. Experimental Section

2.1. Materials. The cellulose samples were kindly donated by Lenzing AG (Austria). The molecular weights stated in Table 1 were given by the supplier and are based on gel permeation chromatography measurements in the mixed solvent dimethylacetamide + LiCl. For our investigations we used bidistilled water.

2.2. Procedures. **2.2.1. Vapor Pressure Measurements.** An automated combination of head space sampling and gas chromatography has been used to determine the vapor pressures of water. Well-defined amounts of the equilibrium gas phase coexisting with the swollen cellulose sample are taken from vials (10 mL) via a septum by means of a syringe and transferred into a gas chromatograph (thermal conductivity detector), which determines the mass of the solvent that was present in the known volume. The details of the procedure have already been reported¹²

2.2.2. Sample Preparation. Cellulose films of approximately 20–25 μm in thickness were prepared by means of the phase inversion process usually employed for the preparation of membranes. In the present case solutions of cellulose in the mixed solvent dimethylacetamide + LiCl were developed, using acetone as a nonsolvent, and washed with water. The complete removal of salt from the membrane was controlled by testing the wash water with AgNO_3 . The membranes were then kept in a surplus of water at 80 °C until they reached constant weight. To check the attainment of swelling equilibrium, the membranes

* Author to whom correspondence should be addressed. E-mail: bernhard.wolf@uni-mainz.de.

Table 1.

		M_n (kg/mol)	M_w (kg/mol)	$U =$ $(M_w/M_n) - 1$
cellulose	particularities			
Solucell 270	least content of hemicelluloses and slightly higher -COOH content	46.8	96	1.05
Solucell 500		82.0	228	1.78
Borregaard 1200	highest content of hemicelluloses	97.3	536	4.51

were repeatedly taken out of the water, cleaned from droplets on the surface by means of tissue, and weighted. After that we have stepwise removed water by vacuum treatment to prepare films of different water contents for the vapor pressure measurements. The establishment of equilibria after such changes in composition takes approximately 1 day; to be on the safe side we always waited at least 2 days. At the end of the vapor pressure measurements the membranes were dried at 60 °C and under vacuum until they reached constant weight to determine the total amount of cellulose.

3. Theoretical Background

3.1. Original Relations. Because of its simplicity and versatility the present theoretical considerations use an extended form of the Flory–Huggins theory, which will be briefly recalled in the next section. The starting point of that concept is the well-known expression¹³ for the Gibbs energy of mixing formulated here for polymer solutions and 1 mol of segments (indicated by a bar over the corresponding quantity) in eq 1

$$\frac{\bar{\Delta G}}{RT} = (1 - \varphi) \ln(1 - \varphi) + \frac{\varphi}{N} \ln \varphi + g(1 - \varphi)\varphi \quad (1)$$

where φ represents the volume fraction of the polymer and N is the number of segments of the polymer (defined as the ratio of the molar volumes of the polymer and the solvent). The first two terms of the above relation constitute the so-called combinatorial term, a hypothetical reference behavior of mixing, whereas all deviations of real systems from that idealized performance are incorporated in the third term. According to the original concept of Flory and Huggins the integral interaction parameter g should only depend on the variables of state but neither on the composition of the mixture nor on the chain length of the polymer.

Due to the difficulties in the direct determination of Gibbs energies, the only practical way to check the validity of eq 1 consists of the measurements of chemical potentials, i.e., by studying phase equilibria, where liquid/liquid and liquid/gas equilibria for the solvent are the most commonly applied options.¹⁴ The following relation holds true for the Gibbs energy of dilution (the chemical potential of the solvent, index 1, in the mixture minus the chemical potential of the pure solvent)

$$\frac{\bar{\Delta G}_1}{RT} = \ln(1 - \varphi) + \left(1 - \frac{1}{N}\right)\varphi + \chi\varphi^2 \quad (2)$$

where χ stands for the original Flory–Huggins interaction parameter.¹³ Equation 2 constitutes the most commonly used basis for the determination of interaction parameters, because $\bar{\Delta G}_1$ is conveniently measurable in terms of osmotic pressures

or vapor pressures. In the latter case the following relation holds true

$$\frac{\bar{\Delta G}_1}{RT} = \ln \frac{p}{p_o} \quad (3)$$

so that χ is given by

$$\chi = \frac{\ln(p/p_o) - \ln(1 - \varphi) - (1 - 1/N)\varphi}{\varphi^2} \quad (4)$$

In the above equations p stands for the equilibrium vapor pressure of the solvent as established above the polymer solution, and p_o is the vapor pressure of the pure solvent. For most systems of practical interest there is no need to use fugacities instead of the actual vapor pressures.

The values of the interaction parameters defined by means of the eqs 1 and 2, respectively, are for a given system normally not identical, because of their composition dependence. The following phenomenological relation permits the interconversion of g and χ

$$\chi = g - (1 - \varphi) \frac{\partial g}{\partial \varphi} \quad (5)$$

The integral interaction parameter g is, for instance, required for the modeling of phase equilibria employing a direct minimization^{15,16} of the Gibbs energy of the system. This method—avoiding the identification of the conditions for which the chemical potentials become identical—is particularly useful for the modeling of multicomponent mixtures or of systems requiring expressions for the description of $\chi(\varphi)$ that are mathematically complicated.

3.2. Extended Relations. Modifications^{17–19} of the relations presented above are required by two characteristic features of chain molecules, which have been neglected in the original considerations. One of them is the fact that the segments of a given linear macromolecule cannot spread out over the entire volume, even in the case of an infinite surplus of solvent (chain connectivity). The other particularity of chain molecules consists of their variability in spatial extension, which enables them to react on changes in their molecular environment (conformational response).

To incorporate the contributions of these two features into the interaction parameter, the dilution process (underlying the interaction parameter χ) is conceptually divided into two clearly separable steps. The first one consists of the opening of contacts between two segments belonging to different polymer molecules by inserting a solvent molecule in between them such that the arrangement of the molecular environment remains unchanged. This step does normally not yet suffice to establish equilibrium, because the macromolecules (and to a lesser extent also the solvent) are able to respond to changes in the neighborhood. It is only during the second step, the conformational rearrangement, that the Gibbs energy of the system acquires its minimum.

One important element of the refined approach consists of the quantification of the effects of chain connectivity. To establish the required parameter we consider the equilibrium between the “microphase” formed by an isolated polymer coil and the sea of pure solvent that surrounds it. In these considerations the equilibrium size of an isolated coil is not—as usual—deduced from entropical considerations (deviation from unperturbed behavior); here the final extension of the chain is obtained by means of the equilibrium condition of phenomenological thermodynamics.

If we denote the volume fraction of segments within such an isolated coil by Φ_o , then the chemical potential of the solvent inside the mixed phase can be formulated by analogy to eq 2 as

$$\frac{\Delta \bar{G}_1}{RT} = \ln(1 - \Phi_o) + \left(1 - \frac{1}{N}\right)\Phi_o + \lambda \Phi_o^2 = 0 \quad (6)$$

The parameter λ defined in this manner constitutes an intramolecular interaction parameter, measuring the effect of opening a contact between two polymer segments belonging to the same macromolecule by the insertion of a solvent molecule in the case of already established equilibrium. Larger Φ_o values require larger λ values to raise the chemical potential of the solvent inside the mixed phase (defined by the extension of the isolated molecule) to the value for the pure solvent (surrounding the coil). More specifically, due to the fact that the volume fraction of segments within the equilibrium coil increases as the molar mass of the polymer declines, the intramolecular interaction parameter λ must assume larger values for shorter chains; in other words, the restrictions of chain connectivity become more stringent than those for higher molar masses where the segments can spread out over considerably larger volumes. Equation 6 yields the following generally valid relation for λ

$$\lambda = \frac{-\ln(1 - \Phi_o) - (1 - 1/N)\Phi_o}{\Phi_o^2} \quad (7)$$

To obtain Φ_o from easily accessible information, we relate it to the intrinsic viscosity of the polymer. Because of the low Φ_o values, which normally lie below 0.01, we may expand the logarithm in eq 7 in a Taylor series and obtain the following simple expression

$$\lambda = \frac{1}{2} + \kappa N^{-(1-a_{\text{KMH}})} + \dots \quad (8)$$

in which a_{KMH} stands for the Kuhn–Mark–Houwink exponent of the corresponding viscosity–molecular weight relationship and κ represents a system-specific constant, containing the pre-exponential factor of this relation.

The second central element of the refined approach consists of the incorporation of the effects stemming from the conformational variability of chain molecules. To quantify these contributions we have introduced a parameter ζ , called conformational response. For the (pseudo-ideal) theta conditions ζ assumes the value of zero. This means that no rearrangement of the segments is required in the second step of dilution discussed above. Positive ζ values contribute favorably and negative values adversely to the mixing tendency of the components.

The considerations outlined above have led to the following expression for the differential interaction parameter χ

$$\chi = \frac{\alpha}{(1 - \nu\varphi)^2} - \zeta(\lambda + 2(1 - \lambda)\varphi) \quad (9)$$

The integral interaction parameter, g , which is required for the direct minimization of the Gibbs energy results in

$$g = \frac{\alpha}{(1 - \nu)(1 - \nu\varphi)} - \zeta(1 + (1 - \lambda)\varphi) \quad (10)$$

The first term of eq 9 represents an early modification¹⁴ of the original Flory–Huggins theory, accounting for the fact that the

surfaces of the solvent molecule and of the polymer segment (of equal volume) are normally different. The parameter α quantifies the effect associated with the opening of a contact between two polymer segments belonging to different macromolecules at infinite dilution. It constitutes the basis of solvent quality and affects the other system-specific parameters, above all the conformational response ζ . The parameter ν accounts for the fact that the shapes of solvent molecules and polymer segments influence the number of intermolecular contacts that can be opened upon the addition of further solvent at higher polymer concentrations; ν is related to, but not identical with, the purely geometrical parameter γ defined as

$$\gamma = 1 - \frac{(s/\nu)_{\text{polymer}}}{(s/\nu)_{\text{solvent}}} \quad (11)$$

where s and ν are surfaces and volumes of the components, respectively. The parameter γ can be easily calculated from tabulated increments for the different chemical units²⁰ in contrast to ν , which measures effective surface to volume ratios and also depends on the particular thermodynamic situation as quantified by α . Some experimental findings indicate that ν might become identical with γ for theta conditions (where $\alpha = 0.5$ and $\zeta = 0$). In this context it is interesting to note that the very unique behavior modeled by the original Flory–Huggins theory is regained by the present approach in the very special case of theta systems, for which $\zeta = 0$ and only for components with the same efficient surface to volume ratio, i.e., $\nu = 0$.

All contributions of the extended approach accounting for chain connectivity and conformational relaxation are contained in the second term of eq 9. According to the above it is obvious that ζ and λ cannot be totally independent of α : To what extent the conformational relaxation contributes to χ will be governed by the flexibility of the polymer chain and by α , the effect characterizing the first step of dilution. Similarly α will also modify the chain connectivity parameter λ , which is primarily determined by N ; in the case of estimating the volume of an isolated coil by means of the intrinsic viscosity ($[\eta]$) this influence of α becomes immediately obvious. Smaller α values lead to larger $[\eta]$ and alleviate the restrictions of chain connectivity because of the larger volume that is available for the segments. According to eq 9 a quantitative description of the thermodynamic behavior of polymer solutions requires four system-specific parameters. However, α and ζ are so closely interrelated for a given class of polymers that one parameter can be eliminated once this functionality is established. In view of the manifold and often complex behavior of such systems the necessity of the remaining three parameters appears reasonable and justified. In any case the new approach has turned out to be helpful to rationalize a number of hitherto incomprehensible experimental observations, such as molecular weight influences up to the polymer melt,²¹ the reasons for the solubility of 1,2-polybutadiene in *n*-hexane and the insolubility of 1,4-polybutadiene in this solvent,²² the existence of two critical points for a binary polymer solution,²³ two different theta temperatures for binary polymer blends,²⁴ and inversions of heat effects with composition for polymer solutions.²⁵

The first example for the usefulness of eq 9 refers to the molecular weight dependence of the second osmotic virial coefficient A_2 . This measure for the pair interactions between the macromolecules is related to χ_o , the interaction parameter in the limit of infinite dilution, by

$$A_2 = \frac{0.5 - \chi_o}{\rho_2^2 \bar{V}_1} \quad (12)$$

In the above relation ρ_2 is the density of the polymer, and \bar{V}_1 is the molar volume of the solvent. Setting $\varphi = 0$ in eq 9 yields the following expression for χ_o

$$\chi_o = \alpha - \zeta\lambda \quad (13)$$

The problem in the area of high dilution consisted of the observation (as already reported by Flory²⁶ years ago) that A_2 may increase with rising M , in contrast to all theoretical considerations. This finding automatically implies that the second osmotic virial coefficient does not necessarily become zero in the limit $M \rightarrow \infty$. Experiment and theory can be reconciled in terms of negative ζ values. According to the present approach A_2 does only exceptionally vanish for infinitely long chains; in normal cases it assumes small but finite (positive or negative) values.

The composition dependence of χ formulated in eq 9 has meanwhile proven very useful for the quantitative description of numerous systems with very diverse dependencies on composition including the passage of extrema.¹⁸ Furthermore, the new approach is capable of explaining the changes in the sign of the heat of dilution with composition observed for several polymer solutions.²⁷ It was also successfully applied for the rationalization of the conditions under which the demixing of polymer/solvent systems becomes anomalous²³ in the sense that they exhibit two different critical points. In the case of polymer blends the new approach predicts well-defined critical compositions (normally realized at different temperatures) in the limit of infinite molar masses of both polymers,²⁴ in contrast to the original Flory–Huggins theory. To the best of the knowledge of the authors the concept accounting for chain connectivity and conformational relaxation provides the tools to describe liquid/liquid and liquid/gas equilibria by means of the same set of parameters for the first time. Furthermore it is able to explain in a straight forward manner the fundamental differences in the solubility of 1,2- and 1,4-polydienes.²²

4. Results and Discussion

4.1. Vapor Pressures and Swelling. The composition dependencies of the equilibrium vapor pressures of water for the three cellulose samples are shown graphically in the next three diagrams. These results display several striking features. First of all they document that cellulose can take up considerably more than 80 vol % water before a second phase, consisting of practically pure water, is segregated. The two-phase area, within which the vapor pressure is identical with that of the pure water, is in Figures 1–3 accentuated by shading. At least as unexpected as the large degree of swelling is the observation that the higher-molecular-weight cellulose samples incorporate more solvent into the polymer-rich phase than the lower-molecular-weight ones. This uncommon increase in mixing tendency with rising molecular weight of the polymer is consistent with the fact that the vapor pressure of water above a 50/50 mixture (v/v) with cellulose is approximately half that of pure water in the case of Solucell 270, whereas it is only about one-third for the other two polymer samples.

Another remarkable feature consists of the pronounced differences in the scattering of the data points for the individual polymer samples. The experimental accuracy is highest for

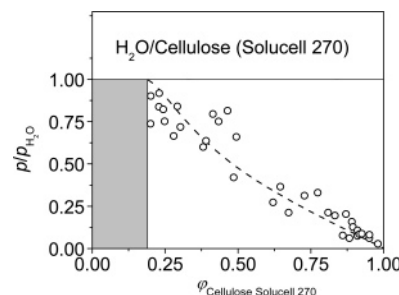


Figure 1. Composition dependence of the vapor pressure of water, divided by the vapor pressure of pure water as a function of the volume fraction of cellulose Solucell 270 at 80 °C. The broken line serves as a guide for the eye only. The two-phase area of the system is given prominence by shading.

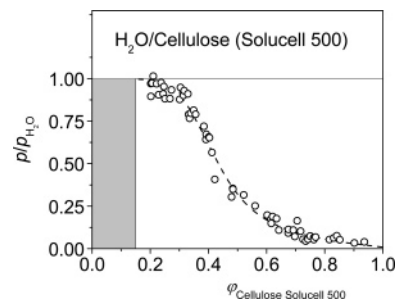


Figure 2. Same as Figure 1 but for cellulose Solucell 500.

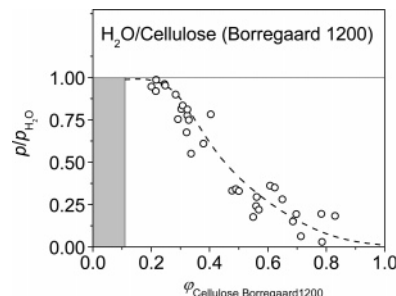


Figure 3. Same as Figure 1 but for cellulose Borregaard 1200.

Solucell 500 and least for Solucell 270. The reasons for these dissimilarities are presently unclear.

4.2. Interaction Parameters and Their Modeling. Out of the three cellulose samples under investigation Solucell 500 yielded the most accurate and Solucell 270 the least precise data. For these reasons the evaluation of vapor pressures with respect to the composition dependence of the interaction parameters by means of eq 4 starts with the former sample and ends with the latter.

The values of the interaction parameters for the water/cellulose system and the range that they cover upon the variation of composition differ extremely from those observed for typical synthetic vinyl polymers, even if the shape of $\chi(\varphi)$ resembles that of the cyclohexane/poly(dimethylsiloxane) system.¹⁸ The fact that practically all vapor pressures yield negative interaction parameters indicates that the interaction between water and cellulose is highly favorable at high polymer concentrations. However, this does not permit the conclusion that the components are completely miscible over the entire range of compositions because it is the shape of the composition dependence of the Gibbs energy that determines the phase state. Demixing sets in as the second derivative of this function becomes negative. The experimentally observed segregation of a second phase upon dilution is obviously due to the pronounced ascent of χ (and consequently g).

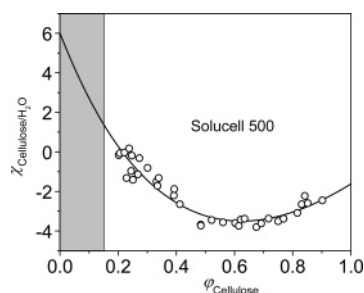


Figure 4. Composition dependence of the interaction parameter for water/cellulose Solucell 500 at 80 °C. The two-phase area is shaded again.

Table 2. Number of Segments, N , of the Different Polymer Samples, Lowest Volume Fraction of Cellulose in Homogeneous Solutions, φ_{swell} , Parameters of Eq 9 Describing the Composition Dependence of χ , and Φ_0 Calculated from λ by Means of Eq 7

	N	φ_{swell}	χ_0	α	ν	ζ	λ	Φ_0
Solucell 270	1630	0.16	3.9	56.8	-0.561	37.9	1.397	0.835
Solucell 500	2940	0.15	6.0	56.8	-0.561	37.9	1.342	0.822
Borregaard 1200	3390	0.11	5.3	56.8	-0.561	37.9	1.361	0.828

The curve shown in Figure 4 corroborates this line of argument and demonstrates that eq 9, established for vinyl polymers, reproduces the experimental findings quantitatively, despite the different nature of cellulose. However, the parameters of this relation that are necessary for such a modeling acquire values, which are up to 100 times larger than those for any other system studied so far, can be seen by comparing the data collected in Table 2 of this work with that of the Tables 1 and 2 in ref 18. For instance, the α value for water/cellulose exceeds 50 and lies well outside the small range around 0.5, which is typical for vinyl polymers. For a better understanding of the particularities of the water/cellulose system it is helpful to calculate the individual contributions of the two steps of dilution and to compare them with the data for an ordinary solvent/polymer system exhibiting approximately the same shape of $\chi(\varphi)$, namely, with the already mentioned cyclohexane/poly-(dimethylsiloxane) (cf. Figure 1 of ref 18). Figure 5 shows the results of this evaluation.

For both types of systems the first term of eq 9 is very adverse for dilution, in contrast to the second term strongly favoring this process. In fact no exception from that feature has hitherto been observed, which indicates that polymer solubility in low-molecular-weight liquids is primarily a consequence of the ability of macromolecules to readjust their conformation to a new environment. These considerations are not in disagreement with the experience that the heat of mixing can be anywhere between endo- and exothermal and may even change its sign with composition.²⁷ The reason is that each step of dilution contributes to the total, experimentally accessible heat effect with its own, concentration-dependent enthalpy change and can thus compose the overall behavior in many different ways.²⁵ In addition to the very dissimilar values of α and $\zeta\lambda$ for the two systems compared in Figure 5 (starting points of the individual contributions at $\varphi = 0$), the composition influences are opposite. In the case of cyclohexane/poly(vinyl methyl ether), behaving in the normal way, the first term of eq 9 becomes more adverse, and that of the second term becomes more favorable as φ rises; the reason lies in the typical values of $\nu > 0$ and $\lambda < 1$. For the water/cellulose system, however, the first term of eq 9 becomes smaller and that of the second term larger, because of $\nu < 0$

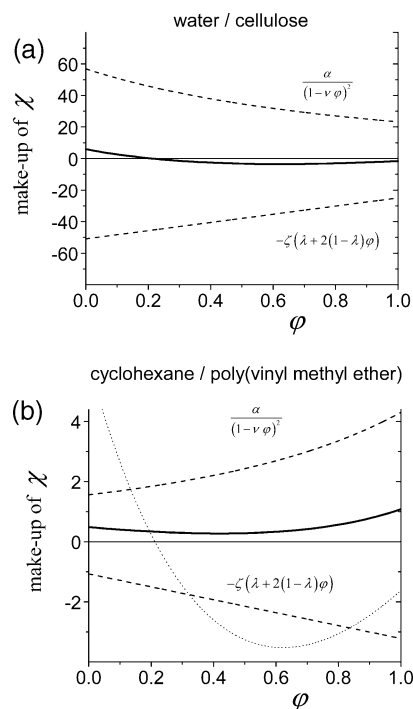


Figure 5. Full lines, $\chi(\varphi)$ as formulated in eq 9; broken lines, individual contributions of the two steps of dilution to the differential interaction parameter. (a) Water/cellulose Solucell 500; (b) cyclohexane/poly(vinyl methyl ether) at 35 °C.¹⁸ To demonstrate the different magnitudes of the effects, the full line of part a is shown as a dotted line in part b.

and $\lambda > 1$. Concerning the reasons for the different signs of these parameters we can presently only speculate. In the case of ν the explanation could lie in the pronounced self-association tendencies of the components, which makes their effective surface to volume ratios very different from the values expected from purely geometrical consideration.²⁰ Similarly the large chain connectivity parameter λ may be caused by the pronounced intramolecular interactions of cellulose, which impede the spreading of segments into a larger volume, even in the case of very long chains.

Let us now come back to the observation that the parameters α and $\zeta\lambda$ assume values on the same order of magnitude for the aqueous solutions of cellulose, as observed with the solutions of vinyl polymers. To check whether the theoretically expected and for vinyl polymers also experimentally witnessed interrelation between α and $\zeta\lambda$ remains valid for the water/cellulose system, we plot the data obtained for Solucell 500 together with that reported earlier¹⁸ in Figure 6.

The interrelation established for vinyl polymers is surprisingly well corroborated by the present finding. In the validation of the results shown in Figure 6 it should be kept in mind that—strictly speaking—each molar mass of the polymer yields its own line, because the factor λ of $\zeta\lambda$ depends on N . For typical vinyl polymers α is small, and the variation of λ (cf. eq 8) can be neglected for most purposes; the lines for high α and large λ may, however, fan out considerably.

The water/cellulose system does not provide direct access to λ via the Kuhn–Mark–Houwink relation. In this case the miscibility gap between the components extends to so minute polymer concentrations that intrinsic viscosities become experimentally inaccessible. Under such unfavorable thermodynamic conditions we must anticipate highly collapsed coils in the limit of vanishing polymer concentration, i.e., large Φ_0 values. To check, whether the λ value obtained from the

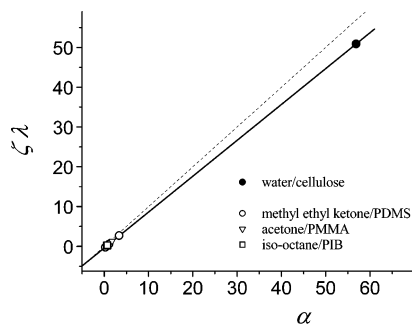


Figure 6. Interrelation between the two terms determining the interaction parameter in the limiting case of infinite dilution (eq 13). The data for the vinyl polymers were reported in ref 18. PDMS, poly(dimethylsiloxane); PMMA, poly(methyl methacrylate);²⁸ PIB, polyisobutylene.

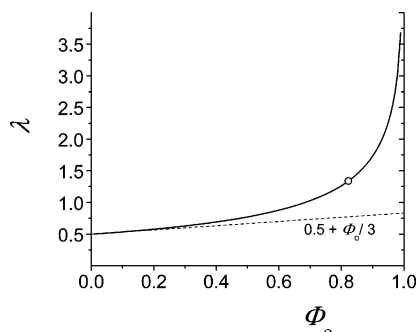


Figure 7. Intramolecular interaction parameter λ as a function of Φ_o , the volume fraction of segments in an isolated polymer coil, calculated according to eq 7, neglecting N with respect to unity. Also shown is the data point for Solucell 500 and the first member of the series expansion of the logarithm in eq 7.

adjustment of the interaction parameters according to eq 9 really yields a Φ_o value that is in accord with that postulated, we determine Φ_o by means of eq 7. The result is shown graphically in Figure 7.

The λ values obtained for Solucell 500 correspond to $\Phi_o \approx 0.82$. This result appears reasonable in view of the observation that water cannot dissolve cellulose to a detectable amount. This observation seemingly contradicts the fact that cellulose incorporates huge amounts of water up to on the order of 80% as demonstrated by Figures 1–3. The two findings can, however, be easily reconciled if one considers the distinct thermodynamic preference of intersegmental contacts over contacts between solvent molecules and polymer segments. This situation leads to a dramatic decrease in the volume fraction, Φ , of the segments of a given cellulose molecule within the volume it occupies at finite polymer concentrations, in comparison with Φ_o , as the polymer concentration becomes sufficiently high. This means that the individual segments of that macromolecule can spread out in space and increase the entropy of the mixture considerably. The reason for this change lies in the incorporation of segments belonging to other cellulose molecules into the realm of a particular coil, which enables the coils to expand. In the (hypothetical) limit of pure liquid cellulose, Φ should have fallen to the value determined by the unperturbed dimensions of the individual coils.

The situation just discussed with respect to the concentration influences of Φ should also play an important role in the context of the mechanical stability of water-swollen cellulose films. The central variables for that property are the degree of coil overlap and the intersegmental interactions, where we have already dealt with the pronounced preference and strength of the contacts between the cellulose segments. The degree of coil overlap

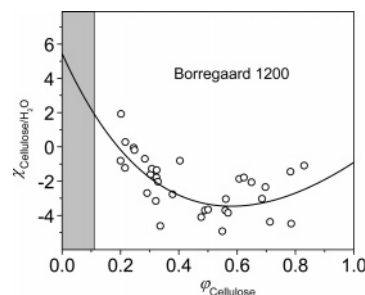


Figure 8. As in Figure 4 but for Borregaard 1200.

assumes its maximum value in the pure state and falls upon the uptake of water. From the observed mechanical stability of the cellulose films down to the onset of the segregation of a second phase consisting of virtually pure water, we may conclude that the addition of water remains rather inefficient until the polymer concentration falls below a critical value; this inference appears reasonable in view of the distinct thermodynamic preference for intersegmental contacts over solvent/segment contacts.

Out of the four parameters contained in eq 9 we have not yet dealt with ν . As already briefly discussed earlier, it accounts for the effective differences in the surface to volume ratios of the components. According to the present measurements the water/cellulose system requires negative values for the correct description of $\chi(\varphi)$. In terms of purely geometrical considerations (eq 11) this would mean that the surface to volume ratio should be smaller for water than that for cellulose segments, which according to the data calculated by means of Bondi's increments²⁰ is not the case. From earlier measurements it is, however, well documented that special effects may overrule simple geometrical considerations. For instance,²² ν is positive for *n*-butane/1,2-polybutadiene, whereas it is negative for *n*-butane/1,4-polybutadiene. This fundamentally dissimilar behavior of two polymers differing only in the spatial arrangement of their chemical units in mixtures with the same solvent may be tentatively explained in terms of differences in the accessibility of their molecular surfaces. It is imaginable that the vinyl side groups of 1,2-polybutadiene shield parts of the segments from contact with *n*-butane. This would explain the different signs of the parameter ν . Concerning the unexpected ν value for water/cellulose one might speculate that the explanation lies in the pronounced self-association tendency of the components; in the case of water, this phenomenon leads to the formation of clusters, which change in size and number with composition.

4.2.1. Borregaard 1200 and Solucell 270. According to the theoretical concept underlying the discussion of the present measurements, all parameters, except for λ , should be independent of the molar mass of the polymer. For that reason we evaluate the measurements with these two cellulose samples setting α , ζ , and ν identical to the parameters obtained for Solucell 500 and adjust λ only. For Borregaard 1200 one obtains $\lambda = 1.361$ in this manner; the individual χ values and their fit according to eq 9 are depicted in Figure 8.

Within the limits of experimental uncertainties, which are particularly large for this highest-molecular-weight sample of cellulose, the experimental findings can be modeled satisfactorily by eq 9. The range of χ values and the shape of the curves plus the extrapolated χ_o are very similar for Solucell 500 and Borregaard 1200. The solutions of the lowest molecular sample Solucell 270 however exhibit noteworthy differences as can be seen from Figure 9.

For cellulose Solucell 270, the composition dependence of χ exhibits a considerably shallower minimum, and χ_o is much smaller than those for the other two samples. Despite these

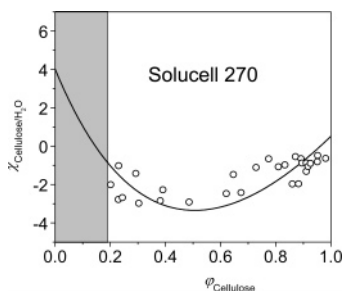


Figure 9. As in Figure 4 but for Solucell 270.

differences it is again possible to describe the curve by adjusting the parameter λ only. Table 2 collects the characteristic data of the three cellulose samples and the parameters of the present evaluation, the corresponding parameters of eq 9 and the Φ_0 values calculated from λ .

4.3. Comparison of Measured and Predicted Swelling. One of the most striking features of the present measurements consists of the observation that the lower-molecular-weight samples of cellulose can take up less water than the higher-molecular-weight ones. For Solucell 270 the polymer-rich phase in equilibrium with practically pure water contains 84 vol % water $[(1 - \varphi_{\text{swell}}) \times 100]$, whereas this value is 89 vol % for Borregaard 1200. This finding implies that the interactions between the components become more favorable with rising chain length, in contrast to the normal behavior.

To rationalize this fundamental difference qualitatively, we recall that α , the central parameter of the present approach, is larger by 2 orders of magnitude for water/cellulose than that for normal systems. This particularity leads to extraordinarily large χ values in the range of high dilution, which impede the formation of dilute solutions, but to very small χ values (which are even more favorable than those for ordinary systems) at large polymer concentrations (cf. Figure 5b). Pure cellulose will take up added water as long as the segments encounter a sufficiently high number of partner segments in their immediate surroundings. In the course of dilution the extent of chain overlap will fall below a critical value, and the cellulose molecules can no longer evade the formation of extremely adverse contacts between its segments and water, which means that phase separation sets in. From simple considerations concerning the chain length dependence of the size of polymer coils it becomes obvious that this critical situation will be reached at higher dilution by larger-molecular-weight samples than by smaller-molecular-weight ones. The just described situation explains why the uptake of water increases as the chain length of cellulose rises.

We are now asking to what extent the interaction parameters obtained from the measured vapor pressures (i.e., from liquid/gas equilibria) predict the influence of N on the swelling of cellulose in water (i.e., liquid/liquid equilibria). To calculate the compositions of the coexisting phases, we have employed the method of direct minimization of the Gibbs energy^{15,16} using the integral interaction parameter g (as formulated in eq 10) by means of the system-specific parameters α , ν , ζ , and λ , collected in Table 2. The outcome of this computation is shown in Figure 10 for the two higher-molecular-weight cellulose samples (excluding the third sample because of its particularities in $\chi(\varphi)$) together with the experimentally determined tie lines. To obtain the functionality $\varphi_{\text{swell}}(N)$ —the full line in Figure 10—we have assumed that Φ_0 increases linearly with the number of segments (connecting the data points for Solucell 500 and Borregaard 1200 by a straight line) and calculated the required λ value by means of eq 7.

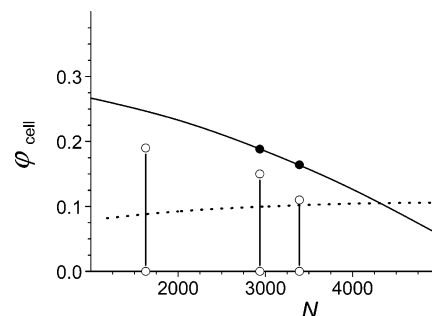


Figure 10. Swelling of cellulose in water as a function of the number of segments N . Open symbols, experimental data; full symbols and full line, calculated by means of eq 1 as described in the text. The dotted line represents the normal swelling behavior and is calculated by means of the original Flory–Huggins theory, setting the interaction parameter equal to 0.54.

The results shown in Figure 10 demonstrate that the miscibility gap of cellulose and water, predicted from the measured vapor pressures by means of the composition-dependent interaction parameters, matches the directly measured swelling behavior surprisingly well. Above all, the information obtained from liquid/gas equilibria, cast into eq 10, predicts the observed diminution of the two-phase region with rising molar mass of the cellulose. The lack of quantitative agreement should not be overestimated, because of the pronounced sensitivity of calculated φ_{swell} with respect to the exact value of the central parameter α , which is demonstrated by the fact that a reduction of α by less than 3% would suffice to lower calculated φ_{swell} to the experimental value.

5. Conclusions

The experimental results and theoretical interpretation presented here indicate the absence of fundamental differences between mixtures of water and cellulose on the one hand and organic solvents and ordinary vinyl polymers on the other hand. These two types of systems distinguish themselves only in the values of the parameters that are required for their quantitative modeling by means a general approach, which allows for the special effects of chain connectivity and conformational variability and yields composition-dependent interaction parameters.

This similarity of systems is, for instance, verified by the observation that the composition dependence of the Flory–Huggins interaction parameter for water/cellulose has the same shape as that for the cyclohexane/poly(vinyl methyl ether) (CH/PVME) system.¹⁸ The main difference between the two systems lies in the range of values that this dependence covers; for the latter system χ varies between approximately 0 and 1, whereas this interval extends from approximately -4 to $+6$ for cellulose and water. That distinction by an entire order of magnitude results from the much larger intermolecular forces between water and cellulose as compared with those between CH and PVME. In terms of α and ζ these dissimilarities manifest themselves as $\alpha \approx 1.5$ and $\zeta \approx 2$ for CH/PVME but $\alpha \approx 55$ and $\zeta \approx 38$ for water/cellulose. In addition to the differences in these leading parameters the values for ν and λ are also rather dissimilar, namely, $\nu \approx 0.35$ and $\lambda \approx 0.50$ for CH/PVME and $\nu \approx -0.56$ and $\lambda \approx 1.35$ for water/cellulose.

The situation described above can be discussed in more detail by the following considerations. For CH/PVME the moderately adverse interaction upon contact formation (positive α) is for all concentrations overcompensated by a sufficiently large favorable conformational relaxation (positive ζ values). The ratio

$\zeta/\alpha \approx 4/3$ is large enough to result in complete miscibility of the components over the entire range of compositions. With water/cellulose however a similar compensation of adverse and favorable effects is no longer feasible at all concentrations because of the much smaller ratio $\zeta/\alpha \approx 2/3$, which is probably caused by the marked chain stiffness of cellulose in solution. For the mixed solvent LiCl plus *N,N*-dimethylacetamide a persistence length of 252 Å was reported,²⁹ i.e., a value that is at least 1 order of magnitude larger than that of ordinary vinyl polymers.

This handicap of cellulose concerning the conformational relaxation creates a problem at low concentrations. Under these conditions the individual cellulose molecules can no longer evade contact with water by contacting other solute molecules; in this case the only way out consists of self-association; i.e., the large α values force the coils to collapse. It is this particular situation that explains the observed anomalous swelling. For a given polymer concentration the degree of coil overlap increases as the molecular weight of cellulose rises. This means that the critical value leading to phase separation is reached at higher dilution.

Acknowledgment. We gratefully acknowledge the financial support of the Deutsche Forschungsgemeinschaft. Furthermore we thank Dr. T. Roeder from the Lenzing AG (Austria) for the donation of the cellulose samples.

List of Symbols

A_2 , second osmotic virial coefficient, eq 12
 $a_{\text{KM}}^{\text{MH}}$, exponent of the Kuhn–Mark–Houwink relation, eq 8
 ΔG , segment molar Gibbs energy of mixing
 ΔG_1 , segment molar Gibbs energy of dilution
 g , integral interaction parameter, eq 1
 N , number of polymer segments
 p , vapor pressure of the solvent above the polymer solutions
 p_o , vapor pressure of pure solvent
 s , molecular surface, eq 11
 V , molar volume
 v , molecular volume, eq 11
 α , contribution of the first step of dilution to the Flory–Huggins interaction parameter χ_o , eq 13
 γ , geometrical factor quantifying the difference in the surface to volume ratios of the components, eq 11
 ζ , conformational response, quantifying the rearrangement of the components in the second step of dilution, eq 9
 κ , parameter of eq 8 containing the pre-exponential factor of the Kuhn–Mark–Houwink relation
 λ , intramolecular solvent/segment interaction parameter for isolated polymer coils, eq 6
 ν , thermodynamically effective difference in the surface to volume ratios of the components, eq 9
 ρ , density
 Φ , volume fraction of the segments belonging to an individual macromolecule within the realm of the corresponding polymer coil

Φ_o , Φ in the limit of infinite dilution of the polymer, eq 6
 φ , volume fraction of the polymer

φ_{swell} , φ of the phase that is in equilibrium with the pure solvent

χ , differential interaction parameter, eq 4

χ_o , differential interaction parameter in the limit of infinite dilution, eq 13

References and Notes

- (1) Newman, R. H.; Davidson, T. C. *Cellulose* **2004**, *11*, 23–32.
- (2) Gordeev, M. E.; Tymbaeva, I. G.; Lebedeva, M. A. *Colloid J.* **2000**, *62*, 140–144.
- (3) Hofstetter, K.; Hinterstoisser, B.; Salmen, L. *Cellulose* **2006**, *13*, 131–145.
- (4) Bochev, A. M.; Kalyuzhnaya, L. M. *Russ. J. Appl. Chem.* **2002**, *75*, 989–993.
- (5) Yakunin, N. A.; Zavadskii, A. E. *Polym. Sci. Ser. A* **2004**, *46*, 634–638.
- (6) Zakharov, A. G.; Pelipets, O. V.; Voronova, M. I.; Prusov, A. N.; Girichev, G. V. *Russ. J. Phys. Chem.* **2004**, *78*, 1508–1510.
- (7) Bismarck, A.; Aranberri-Askargorta, I.; Springer, J.; Lampke, T.; Wielage, B.; Stamboulis, A.; Shenderovich, I.; Limbach, H.-H. *Polym. Compos.* **2002**, *23*, 872–894.
- (8) Platanov, V. A.; Belousov, Y. Y.; Pozhalkin, N. S.; Zenkov, I. D.; Kulichikhin, V. G. *Khim. Volokna* **1983**, *1*, 30–33.
- (9) Chanzy, H.; Nawrot, S.; Peguy, A.; Smith P. J. *Polym. Sci., Polym. Phys. Ed.* **1982**, *20*, 1909–1924.
- (10) Kim, D. B.; Lee, W. S.; Jo, S. M.; Lee, J. M.; Kim, B. C. *Polym. J.* **2001**, *33*, 139–146.
- (11) Navard, P.; Haudin, J. M. *J. Therm. Anal.* **1981**, *22*, 107–118.
- (12) Barth, C.; Horst, R.; Wolf, B. A. *J. Chem. Thermodyn.* **1998**, *30*, 641–652.
- (13) Flory, P. J. *Principles of Polymer Chemistry*; Cornell University Press: Ithaca, NY, 1953.
- (14) Koningsveld, R.; Stockmayer, W. H.; Nies, E. *Polymer Phase Diagrams*, 1st ed.; Oxford University Press: New York, 2001.
- (15) Horst, R. *Macromol. Theory Simul.* **1995**, *4*, 449–458.
- (16) Horst, R. *Macromol. Theory Simul.* **1996**, *5*, 789–800.
- (17) Bercea, M.; Cazacu, M.; Wolf, B. A. *Macromol. Chem. Phys.* **2003**, *204*, 1371–1380.
- (18) Wolf, B. A. *Macromol. Chem. Phys.* **2003**, *204*, 1381–1390.
- (19) Stryuk, S.; Wolf, B. A. *Macromol. Chem. Phys.* **2003**, *204*, 1948–1955.
- (20) Bondi, A. *Physical Properties of Molecular Crystals, Liquids, and Glasses*, 1st ed.; John Wiley & Sons: New York, 1968.
- (21) Jiang, S.; Jiang, W.; Wolf, B. A.; An, L.; Jiang, B. *Macromolecules* **2002**, *35*, 5727–5730.
- (22) Stryuk, S.; Wolf, B. A. *Macromolecules* **2005**, *38*, 812–817.
- (23) Wolf, B. A. *Macromolecules* **2005**, *38*, 1378–1384.
- (24) Wolf, B. A. *Macromol. Chem. Phys.* **2006**, *207*, 65–74.
- (25) Bercea, M.; Wolf, B. A. *Macromol. Chem. Phys.* **2006**, *207*, 1661–1673.
- (26) Flory, P. J.; Mandelkern, L.; Kinsinger, J. B.; Shultz, W. B. *J. Am. Chem. Soc.* **1952**, *74*, 3346–3367.
- (27) Bercea, M.; Wolf, B. A. *Macromol. Chem. Phys.* **2006**, *207*, 1661–1673.
- (28) Kirste, R.; Wild, G. *Makromol. Chem.* **1969**, *121*, 174–183.
- (29) McCormick, C. L.; Callais, P. A.; Hutchinson, B. H., Jr. *Macromolecules* **1985**, *18*, 2394–2401.

BM070174+